View metadata, citation and similar papers at core.ac.uk

brought to you by CORE

provided by ScholarWorks@UNIST

AIP | Physics of Plasmas

Flying mirror model for interaction of a super-intense laser pulse with a thin plasma layer: Transparency and shaping of linearly polarized laser pulses

Victor V. Kulagin, Vladimir A. Cherepenin, Min Sup Hur, and Hyyong Suk

Citation: Physics of Plasmas (1994-present) **14**, 113102 (2007); doi: 10.1063/1.2799169

View online: http://dx.doi.org/10.1063/1.2799169

View Table of Contents: http://scitation.aip.org/content/aip/journal/pop/14/11?ver=pdfcov

Published by the AIP Publishing

Articles you may be interested in

Relativistic effects in the interaction of high intensity ultra-short laser pulse with collisional underdense plasma
Phys. Plasmas **18**, 093108 (2011); 10.1063/1.3633529

Integrated kinetic simulation of laser-plasma interactions, fast-electron generation, and transport in fast ignitiona)
Phys. Plasmas **17**, 056702 (2010); 10.1063/1.3312825

Flying mirror model for interaction of a super-intense nonadiabatic laser pulse with a thin plasma layer: Dynamics of electrons in a linearly polarized external field
Phys. Plasmas **14**, 113101 (2007); 10.1063/1.2799164

Limits for light intensification by reflection from relativistic plasma mirrors
Phys. Plasmas **13**, 093102 (2006); 10.1063/1.2348087

Production of ultrahigh-current-density ion beams by short-pulse skin-layer laser–plasma interaction
Appl. Phys. Lett. **85**, 3041 (2004); 10.1063/1.1797557

Vacuum Solutions from a Single Source

- Turbopumps
- Backing pumps
- Leak detectors
- Measurement and analysis equipment
- Chambers and components

PFEIFFER VACUUM

This article is copyrighted as indicated in the article. Reuse of AIP content is subject to the terms at: http://scitation.aip.org/termsconditions. Downloaded to IP: 114.70.7.203 On: Wed, 12 Nov 2014 01:21:14

Flying mirror model for interaction of a super-intense laser pulse with a thin plasma layer: Transparency and shaping of linearly polarized laser pulses

Victor V. Kulagin[a)]
Center for Advanced Accelerators, KERI, Changwon, 641-120, Republic of Korea

Vladimir A. Cherepenin[b)]
Institute of Radioengineering and Electronics of RAS, Mohovaya 11, Moscow 125009, Russia

Min Sup Hur[c)] and Hyyong Suk[d)]
Center for Advanced Accelerators, KERI, Changwon, 641-120, Republic of Korea

(Received 19 June 2007; accepted 24 September 2007; published online 2 November 2007)

A self-consistent one-dimensional (1D) flying mirror model is developed for description of an interaction of an ultra-intense laser pulse with a thin plasma layer (foil). In this model, electrons of the foil can have large longitudinal displacements and relativistic longitudinal momenta. An approximate analytical solution for a transmitted field is derived. Transmittance of the foil shows not only a nonlinear dependence on the amplitude of the incident laser pulse, but also time dependence and shape dependence in the high-transparency regime. The results are compared with particle-in-cell (PIC) simulations and a good agreement is ascertained. Shaping of incident laser pulses using the flying mirror model is also considered. It can be used either for removing a prepulse or for reducing the length of a short laser pulse. The parameters of the system for effective shaping are specified. Predictions of the flying mirror model for shaping are compared with the 1D PIC simulations, showing good agreement. © *2007 American Institute of Physics*.
[DOI: 10.1063/1.2799169]

I. INTRODUCTION

Theory for interaction of super-intense laser pulses with thin plasma layers (foils) has been rapidly developed in recent years.[1–11] These investigations were triggered both by the availability of the laser pulses with ultrarelativistic amplitudes[12] and by results of the experiments on the high-intensity laser-pulse interaction with thin foils.[13–17] An exact analytical approach likely cannot be developed for a full description of a real plasma layer, and only numerical simulations are possible. However, the main features of the interaction of the laser pulse with the real plasma layer can be described by the approximate phenomenological models, particularly by models containing only one electron sheet.

So far, several theoretical models were developed for description of an interaction of a high-intensity laser pulse with a plasma layer. In these models, transition and reflection of the pulse are of primary interest. The oscillating mirror model[18,19] was used for calculation of harmonics in the field reflected off a semi-infinite plasma. The use of thin foils for laser pulse shaping was proposed for the first time in Ref. 1 and developed as the sliding mirror model in Ref. 2 and 3. Later, this model was used for description of attosecond pulse generation.[20,21] The model based on analytical stationary solutions (with vanishing longitudinal momenta) was developed in Refs. 7 and 8. However, all of these theories have the same defect—they suppose that the longitudinal motion of the plasma-layer electrons vanishes (or at least has amplitude considerably smaller than the laser wavelength). This supposition can be reasonable for semi-infinite solid-density plasma, but for thin plasma layers, it is valid only for small enough amplitudes of the incident laser field (although this amplitudes can be ultrarelativistic).

In this paper, a one-dimensional flying mirror model[22] is developed for description of the interaction of an ultra-intense laser pulse with a thin plasma layer (the term "flying mirror" was first used in Ref. 23). This model contains one electron sheet, and it is self-consistent since it takes into account the self-radiation of the electron sheet, and the Coulomb force of the ion remainder is accounted for. The main difference from existing theories is the possibility for large longitudinal displacements of the electrons (considerably larger than the laser wavelength). The flying mirror model can be considered as an extension of the sliding mirror model for large laser pulse amplitudes, since for small amplitudes they give the same results. Approximate analytical expressions for the transmitted and the reflected fields are derived for the flying mirror model.

The predictions of the developed flying mirror model are compared with the predictions of the sliding mirror model[1–3] and the pure Coulomb model[22] (in which the radiation reaction force is omitted), and also with the one-dimensional particle–in–cell (1D PIC) simulations. From this comparison,

[a)]On leave from Sternberg Astronomical Institute of Moscow State University, Russia. Present address: APRI, GIST, Gwangju 500-712, Republic of Korea. Electronic mail: victorvkulagin@yandex.ru
[b)]Electronic mail: cher@cplire.ru
[c)]Electronic mail: mshur@keri.re.kr
[d)]Present address: APRI and School of Photon Science and Technology, GIST, Gwangju 500-712, Republic of Korea. Electronic mail: hysuk@gist.ac.kr

 © 2007 American Institute of Physics

This article is copyrighted as indicated in the article. Reuse of AIP content is subject to the terms at: http://scitation.aip.org/termsconditions. Downloaded to IP: 114.70.7.203 On: Wed, 12 Nov 2014 01:21:14

we conclude that the flying mirror model describes the transmittance of a real thin plasma layer better than other one-sheet models when the laser pulse amplitude is high enough (and electrons have relativistic longitudinal momenta). The flying mirror model predicts new effects such as dependence of the foil transmittance on time (the electron sheet protracts sharp laser front), resulting in almost complete transparency for large enough laser-pulse amplitude and long enough time. Also, the model shows that the amplitude transmission coefficient depends essentially on the form of the laser pulse envelope.

The removal of the laser pulse pedestal and the reduction of the length for the short laser pulses are also considered with the flying mirror model. Parameters of the system for effective shaping are specified. The pedestals as high as 1/3 of the maximal field amplitude can be almost totally suppressed; also, spiky features in the laser pulses can be separated from a diffuse background. The reduction of the pulse duration can be effective for the short incident pulses with steep enough fronts; during shaping, the asymmetric pulses with a sharp front end and a smooth back end can be produced. The predictions of the flying mirror model for shaping are compared with the 1D PIC simulations showing good agreement.

The paper is organized as follows: In Sec. II, the general mathematical model for radiation and transparency of an ideal electron sheet is considered. In Sec. III, the results for the flying mirror model are compared with the predictions of the sliding mirror model and the pure Coulomb model using the PIC simulations for interaction of a test laser pulse (having a step-like envelope) with a real thin plasma layer. In Sec. IV, the approximate analytical solutions for the transmitted and the reflected fields are derived for the flying mirror model. In Sec. V, the removal of the laser pulse pedestal and the reduction of the laser pulse length are considered using the flying mirror model, and the results are compared with the 1D PIC simulations. In Sec. VI, conclusions are presented.

II. RADIATION FIELD AND TRANSPARENCY OF AN IDEAL ELECTRON SHEET

Let an ideal electron sheet with infinitely small thickness and uniform surface charge density σ have infinite dimensions in the x and y directions. If the movement of the sheet is without rotations and deformations, then all variables depend only on coordinate z and time t, and the movement of the sheet can be described by three components of velocity $\boldsymbol{\beta}=\mathbf{v}/c$ and one coordinate Z.[24]

Charge and current densities for the electron sheet are $\rho(z,t)=\sigma\delta[z-\tilde{Z}(t)]$ and $\mathbf{j}(z,t)=\sigma\mathbf{v}(t)\delta[z-\tilde{Z}(t)]$. Radiation fields of the electron sheet at coordinate z and time t can be obtained with the help of Green function and have the form[22,25,26]

$$\mathbf{E}_{\perp e}(z,t)=-2\pi\sigma\frac{\boldsymbol{\beta}_{\perp}(t')}{1-\beta_z(t')\mathrm{sign}[z-\tilde{Z}(t')]}, \tag{1}$$

$$\mathbf{H}_e(z,t)=\frac{2\pi\sigma\mathrm{sign}[z-\tilde{Z}(t')][\boldsymbol{\beta}_{\perp}(t')\times\mathbf{e}_z]}{1-\beta_z(t')\mathrm{sign}[z-\tilde{Z}(t')]},$$

where $\mathbf{E}_{\perp e}=E_{xe}\mathbf{e}_x+E_{ye}\mathbf{e}_y$, $\mathbf{v}_{\perp}=v_x\mathbf{e}_x+v_y\mathbf{e}_y$, and t' is the retarded time

$$c(t-t')=|z-\tilde{Z}(t')|. \tag{2}$$

If an external plane electromagnetic wave with arbitrary polarization

$$\mathbf{E}(\omega t-kz)=E_0\mathbf{e}_{0\perp}(\omega t-kz) \tag{3}$$

is incident normally upon the ideal electron sheet along the z axis (ω and $k=2\pi/\lambda$ are the frequency and the wave vector of the wave, E_0 is the wave amplitude, and the function $\mathbf{e}_{0\perp}$ describes the wave envelope), then, for the electrons in the sheet, one has the following equations of motion, which take into account the radiation reaction force and the Coulomb ion force:[22]

$$\frac{dp_x}{d\theta}=-a_0e_{0x}-\frac{s\alpha}{\kappa}p_x,\quad \frac{dp_y}{d\theta}=-a_0e_{0y}-\frac{s\alpha}{\kappa}p_y,$$
$$\frac{d\kappa}{d\theta}=\alpha\left(\mathrm{sign}Z-s+\frac{s}{1+p_x^2+p_y^2}\right),\quad \frac{dZ}{d\theta}=\frac{p_z}{\kappa}, \tag{4}$$

where $\kappa=\gamma-p_z=\sqrt{1+p_x^2+p_y^2+p_z^2}-p_z$ and

$$a_0=\frac{|e|E_0}{mc\omega},\quad \alpha=\frac{2\pi\sigma e}{mc\omega}=\frac{2\pi nle^2}{mc\omega}=\pi\frac{\omega_p^2}{\omega^2}\frac{l}{\lambda}. \tag{5}$$

Here, the surface charge density σ of the ideal electron sheet can be calculated through the volume density of electrons, n, and thickness l of the real plasma layer ($\sigma=nl$), and $\omega_p=\sqrt{4\pi ne^2/m}$ is the characteristic plasma frequency (e and m are the electron charge and mass, c is the speed of light in vacuum).

In Eqs. (4), the normalized (dimensionless) momenta are used $p=\tilde{p}/(mc)$, where $\tilde{p}$ is the ordinary dimensional momenta. Besides, the dimensionless time $\tau=\omega t$ and the dimensionless coordinate $Z=k\tilde{Z}$ were introduced (this normalization is applied also to the coordinate z of any point), and $\theta=\tau-Z(\tau)=\omega t-k\tilde{Z}(t)$. For the normalized energy γ and the longitudinal momentum p_z of the electrons in the sheet, one has

$$\gamma=\frac{1+p_x^2+p_y^2+\kappa^2}{2\kappa},\quad p_z=\frac{1+p_x^2+p_y^2-\kappa^2}{2\kappa}. \tag{6}$$

The value for the parameter s specifies the model used for the description of the interaction. If $s=1$, then the flying mirror model is used,[22] which takes into account the radiation of the electron sheet self-consistently; for $s=0$, the pure Coulomb model is addressed, and here, the motion of the electrons is calculated without the action of the self-radiation. The sliding mirror model[1–3] supposes that $s=1$, however it forces p_z to be equal to zero, which gives[22] $\kappa=\gamma=\sqrt{1+p_x^2+p_y^2}$, so the dynamics of the electrons is governed by the equations for p_x and p_y only. It is necessary to note that, for small laser pulse amplitudes $a_0\ll\alpha$, the longi-

This article is copyrighted as indicated in the article. Reuse of AIP content is subject to the terms at: http://scitation.aip.org/termsconditions. Downloaded to IP: 114.70.7.203 On: Wed, 12 Nov 2014 01:21:14

tudinal displacements of the electron sheet are considerably smaller than the laser wavelength λ, so the flying mirror model practically coincides with the sliding mirror model. In this sense, the flying mirror model can be considered as the generalization of the sliding mirror model for the large (with respect to the parameter α) values of the laser field amplitudes.

It is useful to express the radiation fields of the sheet (1) in terms of parameters a_0 and α introduced above. Let the radiation field of the sheet, running to the right (in the positive direction of the z axis), be $\mathbf{E}_-$, and that running to the left (in the negative direction of the z axis) be $\mathbf{E}_+$. From Eqs. (1), one has

$$\mathbf{E}_{\perp\pm}(z,t) = -2\pi\sigma\frac{\boldsymbol{\beta}_\perp(t')}{1\pm\beta_z(t')} = \frac{\alpha}{a_0}\frac{\boldsymbol{p}_\perp(t')}{\kappa_\pm(t')}E_0. \tag{7}$$

Here, $\kappa_+=\gamma+p_z=(1+p_x^2+p_y^2)/\kappa$ and $\kappa_-=\gamma-p_z=\kappa$. For the right-running radiation of the sheet, we have already made the deformation of the time axis required by Eq. (2) during transformation to the variable θ. So the radiation field to the right at the point (z_0,τ_0) has the following form in the laboratory frame:

$$\mathbf{E}_{\perp-}(z_0,\tau_0) = \left(\frac{\alpha}{a_0}\frac{\boldsymbol{p}_\perp(\theta)}{\kappa(\theta)}E_0\right)_{\theta=\tau_0-z_0}. \tag{8}$$

For the left-running radiation field, it is necessary to account for the deformation of the time axis during transfer from the system with independent variable $\theta=\tau-Z(\tau)$ to the system with independent variable $\theta_+=\tau+Z(\tau)$:

$$\theta+2Z(\theta)=\theta_+. \tag{9}$$

In the system with independent variable θ_+, the expression analogous to Eq. (8) is valid. Then, from Eqs. (8) and (9), one can obtain

$$\begin{aligned}\mathbf{E}_{\perp+}(z_0,\tau_0) &= \left(\frac{\alpha}{a_0}\frac{\boldsymbol{p}_\perp(\theta_+)}{\kappa_+(\theta_+)}E_0\right)_{\theta_+=\tau_0+z_0}\\ &= \left(\frac{\alpha}{a_0}\frac{\boldsymbol{p}_\perp(\theta)\kappa(\theta)}{1+p_\perp^2(\theta)}E_0\right)_{\theta+2Z(\theta)=\tau_0+z_0}.\end{aligned} \tag{10}$$

Multiplying expressions (8) and (10) by $|e|/(mc\omega)$, one can rewrite them in the form

$$\begin{aligned}\mathbf{a}_{\perp-}(z_0,\tau_0) &= \left(\frac{\alpha\boldsymbol{p}_\perp(\theta)}{\kappa(\theta)}\right)_{\theta=\tau_0-z_0},\\ \mathbf{a}_{\perp+}(z_0,\tau_0) &= \left(\frac{\alpha\boldsymbol{p}_\perp(\theta)\kappa(\theta)}{1+p_\perp^2(\theta)}\right)_{\theta+2Z(\theta)=\tau_0+z_0}.\end{aligned} \tag{11}$$

For the transmitted field, one has [note that the incident external field $\mathbf{E}$ is the right-running according to Eq. (3)]

$$\mathbf{a}_t = \frac{|e|\mathbf{E}_t}{mc\omega} = a_0\mathbf{e}_{0\perp}+\mathbf{a}_{\perp-}. \tag{12}$$

The fields $\mathbf{a}_{\perp\pm}$ and $\mathbf{a}_t$ are normalized by the frequency ω of the incident field although the frequency bandwidth of the radiation fields can be wide enough.

If $a_0 \ll \alpha$ and the longitudinal motion of the sheet is negligible then $\kappa_+=\kappa_-=\gamma$ in Eqs. (7) and the Doppler effect is inessential, so the left-running and the right-running radiations of the sheet are equal to each other. This is the so-called viscous regime[22] of laser pulse interaction with a thin plasma layer, which is characterized by a high reflectance of the plasma layer. For this regime, the solutions found before[3,27] are valid. However, for large field amplitudes $a_0 \geqslant \sqrt{2(\kappa_0^2+\alpha^2)}$ ($\kappa_0\simeq 1$ is the value for κ at the beginning of the longitudinal oscillation cycle, cf. Sec. IV below), the electrons participate in large longitudinal oscillations, which amplitude can be considerably larger than the laser wavelength λ. This is the flying regime of interaction[22] characterized by a high transmittance of the plasma layer. The right-running and the left-running radiations of the electron sheet will be different here due to the Doppler effect. For the reflected wave (left-running radiation of the electron sheet), there will be a large phase modulation determined by Eq. (9), and the phase variable cannot be considered as slow. On the other hand, the right-running radiation of the electron sheet has the slowly changing phase [cf. Eqs. (8) and (11)]. Therefore, the reflected wave will be enriched with harmonics of the external wave frequency in a great amount, while the transmitted wave will be relatively poor in harmonics.

The enrichment of the reflected radiation with harmonics is also apparent from the highly nonsinusoidal character of the reflected wave inside a period of the laser field. Actually, according to Eqs. (11), the amplitude of the reflected field is large when $p_\perp(\theta)\sim 1$. For smaller or larger values of $p_\perp(\theta)$, the amplitude of the reflected wave decreases. So there is a strong amplitude modulation of the reflected field inside the laser period that indicates the presence of high harmonics.

Another difference between the left-running and the right-running radiations of the ideal electron sheet in the case of large longitudinal displacements is the amplitude dependence on time. Actually, according to Eqs. (11), at the beginning of longitudinal oscillation cycle when the parameter κ is smallest,[22] the right-running radiation of the sheet has the largest amplitude, then the amplitude decreases. The left-running radiation of the ideal electron sheet (the reflected wave) has, in some sense, opposite behavior since its amplitude is the smallest at the beginning of the longitudinal oscillation cycle and then grows up together with the parameter κ.

III. COMPARISON OF THE MODELS IN THE HIGH-TRANSMITTANCE (FLYING) REGIME USING TEST LASER PULSE WITH A STEP-LIKE ENVELOPE

For a comparison of predictions for three one-sheet models (flying and sliding mirrors models and pure Coulomb model) with the results of the 1D XOOPIC[28] simulations, we used a test laser pulse with a step-like envelope and $a_0=10$. Since the flying regime of interaction is the most interesting, the laser pulse amplitude was considerably greater than $\alpha=2$. In Fig. 1, the transmitted radiations (right-running) for three models and for the PIC simulations are presented. The plasma layer has density $n_0\simeq 7\times 10^{22}$ cm^{-3} and thickness l

This article is copyrighted as indicated in the article. Reuse of AIP content is subject to the terms at: http://scitation.aip.org/termsconditions. Downloaded to IP: 114.70.7.203 On: Wed, 12 Nov 2014 01:21:14

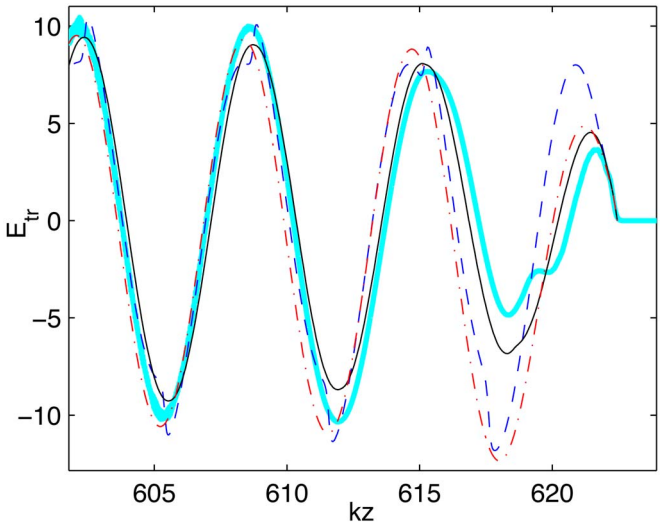

FIG. 1. (Color online) Comparison of the field transmitted through an ideal electron sheet in different models of interaction: thick solid line (cyan) is the PIC simulations result, thin solid line (black) is the flying mirror model calculations, dashed-dotted line (red) is the pure Coulomb model predictions, and dashed line (blue) is the sliding mirror model results. The incident laser pulse has a step-like envelope with $a_0=10$ and $\varphi_0=0$, $\alpha=2$.

$=0.01\lambda$, which is considerably smaller than the laser wavelength. For the PIC simulations, the moving window technique was used, there were 2000 grid points on λ in the longitudinal direction and 200 particles per cell. Since many electrons are carried away by the laser pulse in the flying regime, the transmitted field is presented after about 100 laser periods from the beginning of the interaction, when most of the electrons turned back. From Fig. 1, one can conclude that the flying mirror model describes the flying regime of the interaction of the laser pulse with the plasma layer in the best way. The pure Coulomb model does not describe the front of the transmitted pulse properly since the second half-period has too big amplitude. Besides, this model is not self-consistent, therefore the drift term in the transverse momenta of the electrons does not decrease with time,[22] giving evident zero-frequency component of the transmitted spectrum. The sliding mirror model gives also wrong amplitude for the two first half-cycles of the transmitted pulse, besides, the transmitted radiation is overly enriched with harmonics. So below, we shall consider in more details the flying mirror model only.

IV. RADIATION AND TRANSPARENCY OF THE ELECTRON SHEET IN THE FLYING MIRROR MODEL

A. High-transmittance (flying) regime

The dynamics and the radiation of the electron sheet are essentially different in the flying regime, when $a_0>\sqrt{2(\kappa_0^2+\alpha^2)}$, and in the viscous regime, when $a_0<\sqrt{2(\kappa_0^2+\alpha^2)}$.[22] Let the external field be linearly polarized,

$$a_0 e_{0x}(\theta)=a_0(\theta)\sin(\theta+\varphi_0), \tag{13}$$

where the amplitude $a_0(\theta)$ of the external field is a slowly varying function in comparison with $\sin(\theta+\varphi_0)$, and $\varphi_0=\text{const}$ is the initial phase of the external field. The approximate solutions of Eqs. (4) for p_x and κ can be obtained in the flying regime with the method of the slowly varying envelope,[22]

$$p_x=p_0\left[\cos(\theta+\varphi_0+\varphi)-\exp\left(-\frac{\alpha\theta}{\kappa}\right)\cos(\varphi_0+\varphi)\right],$$

$$p_0=\frac{a_0\kappa}{\sqrt{\alpha^2+\kappa^2}},\quad \tan\varphi=\frac{\alpha}{\kappa}, \tag{14}$$

$$\kappa=\sqrt{\left(\sqrt{\kappa_0^2+\alpha^2}+\alpha\int_0^\theta\frac{d\theta}{\sqrt{a_0^2+1}}\right)^2-\alpha^2}.$$

These solutions are valid inside some longitudinal oscillation cycle, which is defined by the condition $Z>0$ and has the following period:[22]

$$\theta_l=\frac{\sqrt{a_0^2+1}}{\alpha\sqrt{\kappa_0^2+\alpha^2}}\left(\frac{a_0^2}{2}-\kappa_0^2-\alpha^2\right). \tag{15}$$

The flying regime is characterized by the large values of the period for longitudinal oscillations, $\theta_l\gg 2\pi$, and by the large longitudinal displacements $Z_{\max}\sim\theta_l/2\gg k\lambda$. The right-running radiation of the sheet has the following form according to Eqs. (11) and (14),

$$\mathrm{a}_{\perp-}(\tau_0,z_0)=\left(\frac{a_0\alpha}{\alpha^2+\kappa^2}\left\{\kappa\left[\cos(\theta+\varphi_0)-\exp\left(-\frac{\alpha\theta}{\kappa}\right)\cos\varphi_0\right]-\alpha\left[\sin(\theta+\varphi_0)-\exp\left(-\frac{\alpha\theta}{\kappa}\right)\sin\varphi_0\right]\right\}\right)_{\theta=\tau_0-z_0}, \tag{16}$$

and, for the transmitted field, one has from Eqs. (12) and (16)

$$\begin{aligned}\mathrm{a}_t(\tau_0,z_0)&=a_0\sin(\theta+\varphi_0)+\mathrm{a}_{\perp-}\\&=\left(\frac{a_0\kappa}{\sqrt{\alpha^2+\kappa^2}}\sin(\theta+\varphi_0+\varphi)\right)_{\theta=\tau_0-z_0}\\&\quad-\left(\frac{a_0}{\alpha^2+\kappa^2}\left[\alpha\kappa\exp\left(-\frac{\alpha\theta}{\kappa}\right)\cos\varphi_0-\alpha^2\exp\left(-\frac{\alpha\theta}{\kappa}\right)\sin\varphi_0\right]\right)_{\theta=\tau_0-z_0},\end{aligned} \tag{17}$$

where the terms with exponential multipliers originate from the drift motion of the sheet [cf. the terms with exponential multipliers in the first equation of the system (14)] and have to be accounted for only for small values of θ.

In Fig. 2, the transmitted field through the electron sheet ($\alpha=2$) is presented for an incident laser pulse with a step-like amplitude $a_0=10$. The thick cyan line represents the XOOPIC simulations for the transmitted field (parameters of simulations are the same as in Fig. 1), while the thin blue

This article is copyrighted as indicated in the article. Reuse of AIP content is subject to the terms at: http://scitation.aip.org/termsconditions. Downloaded to IP: 114.70.7.203 On: Wed, 12 Nov 2014 01:21:14

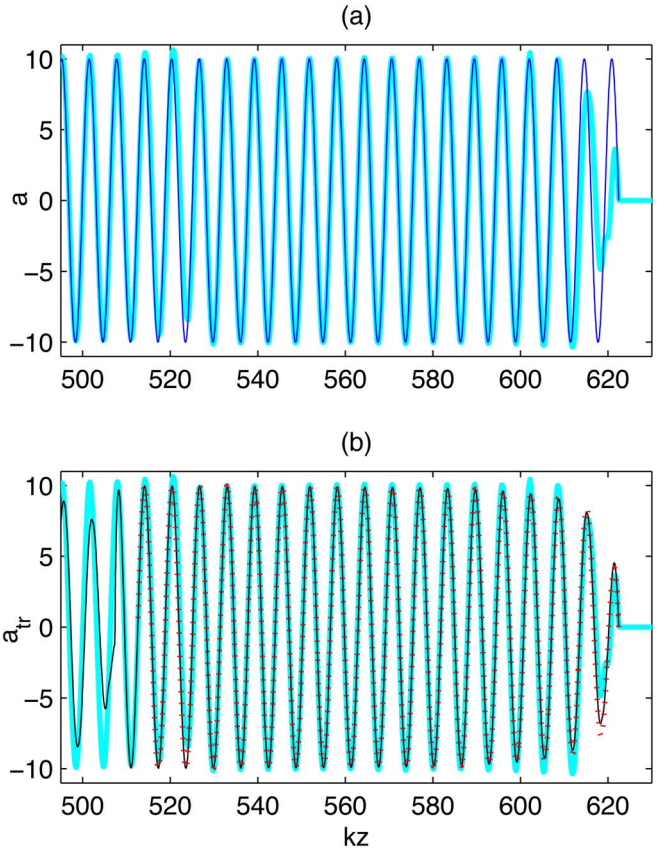

FIG. 2. (Color online) Transmitted field through the electron sheet for a step-like incident laser pulse with the amplitude $a_0=10$ ($\alpha=2$ and $\varphi_0=0$, flying regime): (a) thin blue line is the field of the incident laser pulse and thick cyan line is the transmitted field obtained in the XOOPIC simulations; (b) thick solid line (cyan) is the XOOPIC simulations [same as in (a)], thin solid line (black) is the numerical solution of Eqs. (4) and (12), and dotted line (red) is the approximate analytical solution according to expression (17).

line in Fig. 2(a) is the field of the incident laser pulse and the thin black line in Fig. 2(b) is the transmitted field calculated from the numerical solution of Eqs. (4) substituted into Eq. (12). The dotted red line in Fig. 2(b) is the approximate analytical solution according to expression (17). One can conclude that the matching of the numerical solution for the transmitted field from Eqs. (4) and (12) and the approximate analytical values from Eq. (17) is good enough for the first longitudinal oscillation.

So the modification of the transmitted field is due to the amplitude modulation of the incident field according to the amplitude transmission coefficient

$$t_a = \frac{\kappa}{\sqrt{\alpha^2+\kappa^2}} \tag{18}$$

and also the phase modulation with the phase φ, defined by Eq. (14) (note that this result is valid only[22] for $\theta_l \gg 2\pi$ and when the sheet coordinate $Z>0$).

Equations (17) and (18) show that at the beginning of longitudinal oscillation cycle, when κ is small, the right-running radiation of the sheet compensates the incident external field to the right of the sheet in a great amount (for $\alpha \gg 1$). Therefore, the electron sheet with $\alpha \gg 1$ is almost opaque at the beginning of longitudinal oscillation cycle, with transmittance about α^{-1}. However, then the phase of the sheet radiation changes and the amplitude of the radiation decreases, so the compensation of the incident field also decreases. For large values of κ, the radiation of the sheet has small amplitude, and it is in quadrature with the incident field so the compensation tends to zero. Substituting the value for κ from Eq. (14) into Eq. (18), one can estimate the time dependence of the amplitude of the transmitted field in the case of an incident wave with the step-like amplitude a_0,

$$(a_t)_{\text{amp}} = \frac{a_0\kappa}{\sqrt{\alpha^2+\kappa^2}} = \frac{a_0\theta}{\sqrt{\theta^2+a_0^2}}, \tag{19}$$

where the approximation $\kappa \simeq \alpha\theta/a_0$ is used for the parameter κ (this approximation is valid for $\alpha \gg \kappa_0$ and $\theta > a_0$). So the characteristic time for the front duration of the transmitted field can be estimated as $\theta_{\text{fr}}=a_0$ for the step-like incident pulse. This means that, in the flying regime, the electron sheet protracts the front, and for $a_0 \gg 1$ this effect can be essential. Using also the approximate expression from Eq. (15) for the period of the longitudinal oscillations $\theta_l \simeq a^3/(2\alpha^2)$, valid for $\alpha > \kappa_0$ and $a_0 \gg \alpha\sqrt{2}$, one can estimate the maximum value of the transmission coefficient,

$$(t_a)_{\max} = \frac{a_0^2}{\sqrt{a_0^4+4\alpha^4}} \approx 1 - \frac{2\alpha^4}{a_0^4}, \tag{20}$$

which can be very close to unity. Such a transmission is achieved in times $\theta \sim \theta_l$.

The protraction of a sharp laser front is also evident from the PIC simulations of Fig. 2. However, the transmittance switch from opacity to transparency is more sharp for the real plasma layer then for the ideal electron sheet in the flying mirror model [cf. the amplitudes of the third, fourth, etc., half-cycles in Fig. 2(b) for the PIC simulations and the numerical calculations]. This occurs because the transmittance of the ideal electron sheet can increase only due to the suppression of the self-radiation of the sheet by the increasing κ value according to Eq. (11) (individual mechanism in Ref. 22 for decrease of the sheet radiation). For the real plasma layer, there is in addition another physical mechanism for the increasing the transmittance, namely the destroying of the layer by the laser pulse. Actually, a laser half-cycle with large enough amplitude can carry away all electrons from the ion remainder and accelerate them to relativistic velocities.[29,30] This feature is absent in the semi-infinite plasma, where the Coulomb forces are strong enough to confine the electrons. The electrons, which were carried away by the laser pulse, gradually turn back and increase the transparency of the remaining layer (cooperative mechanism in Ref. 22 for a decrease of the plasma layer radiation). In this sense, for large laser field amplitudes, the flying mirror model is adequate for the description of the laser pulse interaction with the real thin plasma layer only while the thickness of the layer remains considerably smaller than λ, i.e., for transmission of the pulse front. For the body of the laser pulse, the flying mirror model gives only the lower boundary for the transmittance.

This article is copyrighted as indicated in the article. Reuse of AIP content is subject to the terms at: http://scitation.aip.org/termsconditions. Downloaded to IP: 114.70.7.203 On: Wed, 12 Nov 2014 01:21:14

It is interesting also to note that, at the end of the first longitudinal oscillation cycle, there are sharp changes in amplitude and phase of the transmitted field [near $kz \simeq 505$ in Fig. 2(b)] according to Eqs. (4) and (12). The same changes can be seen in the PIC simulations in Fig. 2 near $kz \simeq 520$, when most of the electrons returns to the ions position. The values for the longitudinal oscillation cycle from numerical calculations and from the PIC simulations are close enough (120 and 105 correspondingly), and these values agree well with the analytical estimation from Eq. (15), which gives $\theta_l \simeq 100$.

So the transmission of the electron sheet in the flying regime is not only amplitude-dependent,[1–3] but also time-dependent. Besides, it depends essentially on the form of the pulse envelope according to Eqs. (14) (actually, the estimate (20) is valid for any long pulse, if the amplitude weakly changes during the period of the longitudinal oscillation of the sheet).

It is interesting to note that, in some cases, the transmission of the electron sheet does not depend on the value of α, so that the sheets with different parameter α have the same transparency in the flying regime. One such case is realized when the parameter α is large: $\alpha \gg \kappa_0$ (in fact, this is practically equivalent to $\alpha \gg 1$ since $\kappa_0 \simeq 1$). Then, for the transmission of the sheet, one has from Eqs. (14) and (18) [we do not require now the validity of inequality $\theta > a_0$ as in Eq. (19)]

$$t_a \simeq \frac{\psi(\theta)}{\sqrt{1+\psi^2(\theta)}}, \tag{21}$$

where the function $\psi(\theta)$ is defined by the envelope of the external pulse only,

$$\psi(\theta) = \sqrt{\left(1+\int_0^\theta \frac{d\theta'}{\sqrt{a_0^2+1}}\right)^2 - 1}. \tag{22}$$

In another such case, the parameter α can be small ($\alpha < \kappa_0$), but the time θ has to be large enough. Thus, for the step-like amplitude a_0 of the external field and $\theta > a_0\kappa_0/\alpha$, one can recover the transmission coefficient corresponding to Eq. (19), so the transmission practically does not depend on α for large enough time. Physically, this is due to the growth of the parameter κ that suppresses the own radiation of the sheet.

It is necessary to keep in mind, of course, that the conclusions of this section are valid for the case $Z > 0$ and $\theta_l \gg 2\pi$; for example, when $a_0 < \alpha\sqrt{2}$ the situation changes drastically.

B. High-reflectance (viscous) regime

In the viscous regime with $a_0 \leqslant \sqrt{2(\kappa_0^2+\alpha^2)}$, the parameter κ can be approximately defined by the equation[22] $\kappa = \sqrt{1+p_x^2}$. Then, for the transverse momentum of the electron sheet, one has (note that the same equation is used in the sliding mirror model[1–3])

$$\frac{dp_x}{d\theta} = -a_0 e_{0x} - \frac{\alpha}{\sqrt{1+p_x^2}} p_x. \tag{23}$$

Here, the solution for the transverse momentum p_x of the electron sheet can be also taken in the form, defined by the first equation of the system (14), however the drift term can be omitted now (the drift term in this case modifies the dynamics of the electron sheet only during a short interval of time, which is considerably smaller than the period of the laser field). For p_0 and φ, the method of slowly varying envelope gives[22]

$$p_0^2[1+\alpha^2 f(p_0)^2] = a_0^2, \quad \tan\varphi = \alpha f(p_0), \tag{24}$$

and the function $f(p_0)$ is defined from the following integral (with p_0 to be considered as constant in it):

$$f(p_0) = \frac{1}{\pi}\int_0^{2\pi} \frac{\cos^2\theta d\theta}{\sqrt{1+p_0^2\cos^2\theta}}. \tag{25}$$

Using an analytic approximation $f(p_0) \approx (1+p_0^2)^{-1/2}$, one can obtain[22]

$$p_0^2 = \frac{\sqrt{(a_0^2-\alpha^2-1)^2+4a_0^2}+a_0^2-\alpha^2-1}{2}. \tag{26}$$

It is interesting to note that just the same expression was obtained earlier[3] for the case of a circularly polarized laser pulse, which was, however, exact (inside the averaging method) for the circular polarization.

Longitudinal motion is inessential for the viscous regime, so the left-running and the right-running radiation fields for the sheet are equal, according to Eqs. (11), and are defined just by the parameter p_0:

$$a_{\perp\pm} = \frac{\alpha p_x(\theta)}{\sqrt{1+p_x^2(\theta)}}, \tag{27}$$

where $\theta = \tau_0 \pm z_0$ [the upper (lower) sign is valid for the left (right) running radiation field]. It is obvious that the radiation field can be severely enriched with harmonics of the laser frequency, if p_x becomes greater than unity for some moments of time.

Having in mind the shaping of the incident laser pulses, let us consider in more details the field, transmitted by the electron sheet and defined by Eq. (12). Comparing Eqs. (12), (23), and (27), one can obtain for the transmitted field at the fundamental frequency of the laser light (excluding higher harmonics)

$$a_t = -\frac{dp_x}{d\theta} = p_0 \sin(\theta+\varphi_0+\varphi), \tag{28}$$

where the last equality is derived from Eqs. (14) and the drift term is omitted (p_0 and φ should be considered as constants during differentiation).[22] So the amplitude transmittance t_a of the electron sheet at the fundamental frequency is defined in this regime by the expression

$$t_a = \frac{p_0}{a_0}, \tag{29}$$

and the electron sheet transparency does not dependent directly on time contrary to the flying regime case.

This article is copyrighted as indicated in the article. Reuse of AIP content is subject to the terms at: http://scitation.aip.org/termsconditions. Downloaded to IP: 114.70.7.203 On: Wed, 12 Nov 2014 01:21:14

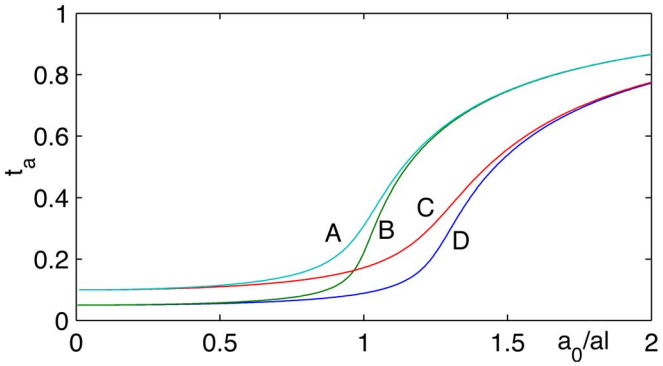

FIG. 3. (Color online) Transmittance coefficient t_a of the electron sheet in the viscous regime for the fundamental frequency ω: approximation from Eq. (26) for $\alpha=10$, A, and $\alpha=20$, B; numerical calculation from the system (24) for $\alpha=10$, C, and $\alpha=20$, D.

For analytic estimates, the approximation for p_0 according to Eq. (26) can be used. It is possible to distinguish three intervals for parameter a_0 giving different dependence for transmittance t_a.

In the first interval, a_0 is small: $a_0 < \alpha - 1$. Then, estimation of expression (26) gives for transmittance $t_a \simeq \alpha^{-1}$. So for a large enough value of parameter α and small enough a_0, which can be, however, ultrarelativistic, the electron sheet reflects almost all radiation at the fundamental frequency according to the results of Refs. 1–3 (higher harmonics, of course, can be radiated by the electron sheet to the left and to the right).

In the second interval, $\alpha - 1 \leqslant a_0 \leqslant \alpha + 1$. In this case, $t_a \simeq 1/\sqrt{\alpha}$ so the transmittance is increased with respect to the first interval. Note that this interval is short for $\alpha \gg 1$.

And at last, for the third interval, $\alpha + 1 \leqslant a_0 \leqslant \alpha\sqrt{2}$. For this interval, $t_a \simeq \sqrt{1-(\alpha^2+1)/a_0^2}$ so the transmittance can be large enough. For further increase of parameter a_0, the flying regime starts and the transmittance becomes time-dependent (cf. Sec. IV A).

The comparison of the electron sheet transmission in the viscous regime for the numerical solutions of Eq. (24) and the approximate solution according to Eq. (26) is presented in Fig. 3 for $\alpha=10$ and 20.

C. Intermediate cutting regime

For $a_0 \sim \alpha\sqrt{2}$, the period θ_l of the longitudinal oscillations of the sheet is about the period of the external wave, and the radiation field of the sheet has complicated structure depending on the ratio of these periods (this regime can be called cutting). This situation is presented in Fig. 4 for $a_0 = 7.7$ and $\alpha=5$, where the radiation of the sheet and the transmitted field are presented. Actually, the fields look chaotic in this case.

It is interesting to note that not only the peaks of the reflected radiation can exceed the amplitude of the incident external field, but the peaks of the transmitted field can also do so. This is due to the very abrupt decrease of the parameter κ to the values less than unity at the end of each longitudinal oscillation cycle,[22] while the momentum p_x preserves its amplitude of oscillation.

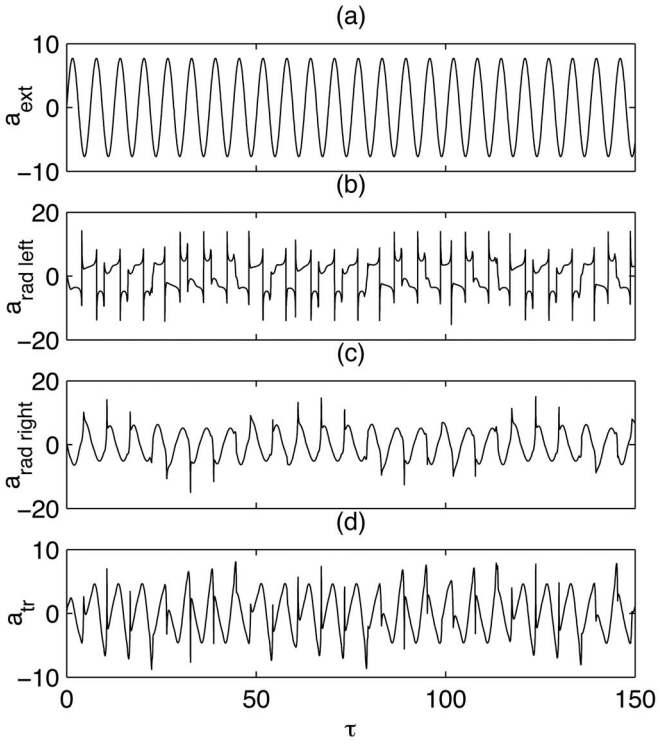

FIG. 4. The left (b) and the right (c) running radiations and the transmitted field (d) of the electron sheet in the field of an intense electromagnetic wave (a) with the step-like amplitude $a_0=7.7$ for $\alpha=5$ and $\varphi_0=0$ (cutting regime), calculated using the flying mirror model. Radiation of the sheet is referred to the point $z_0=0$.

From the PIC simulations for this case, there is one physical effect, which is not predicted by the flying mirror model. Actually, after some time of interaction in the cutting regime (and even in the viscous regime with $a_0 \leqslant \alpha$), the transparency of the plasma layer suddenly increases to almost 100%. This transition is accompanied by the destruction of the plasma layer, more exactly, the thickness of the plasma layer increases by many times with corresponding decrease of the electron density, electrons become to move chaotically with the relativistic longitudinal momenta. Apparently, when the energy of the electrons achieve some threshold, their radiation become to add non-coherently that results in the sharp decrease of the right-going radiation of the plasma layer and corresponding increase of the transmitted amplitude (since the right-going radiation of plasma does not compensate the external field to the right of the plasma layer now). This sudden change in transparency occurs earlier when the ratio a_0/α is higher. The use of this effect for the shaping of very long laser pulses (hundreds of femtoseconds) will be considered elsewhere.

V. SHAPING OF THE INCIDENT LASER PULSES

The switch of the transmittance of a thin plasma layer related with nonlinear effects[1–3] and with destruction of the plasma layer can be used for effective shaping of the incident laser pulses. According to the previous sections, the front part of the linearly polarized laser pulse with $a_0 \leqslant \sqrt{2(\kappa_0^2+\alpha^2)}$ is strongly reflected (the maximal suppression

This article is copyrighted as indicated in the article. Reuse of AIP content is subject to the terms at: http://scitation.aip.org/termsconditions. Downloaded to IP: 114.70.7.203 On: Wed, 12 Nov 2014 01:21:14

of the transmitted pulse during this interval is proportional to $1/\alpha$), and the remaining part of the laser pulse is transmitted.

Let us at first define the possible range of parameters when the shaping of the external laser pulse by the electron sheet is the most efficient. The first parameter, which can be varied for optimizing the shaping, is the maximum amplitude $a_{\max}$ of the laser pulse, which can be changed by additional focusing. Another possible variable parameter is the value of α for the foil. Actually, the parameter α defines the point of the transmittance switch and the suppression of the transmitted field in the opacity regime. When the parameter α is small (smaller than 1), the parameter κ grows up very slowly,[22] and the sheet radiates for a long time. Besides, the radiation of the electron sheet has small amplitude for small values of α so the modification of an external field is small (the transmitted field is about the incident one). Therefore, in the case of $\alpha<1$, the shaping of the laser pulse by the electron sheet is ineffective, and, for shaping, $\alpha>1$ is necessary. Then, taking into account that $\kappa_0 \simeq 1$, one can conclude that the switch of the transmission for the electron sheet will be near $a_{0s} \approx \alpha\sqrt{2}$.

On the other hand, a very large value of the parameter α is also inappropriate for the shaping because, in this case, the transmittance switch will be around relatively large laser pulse amplitudes $a_{0s} \approx \alpha\sqrt{2}$, and the front of the transmitted pulse will have large duration about the value of $\theta_f \simeq a_{0s} \simeq \alpha\sqrt{2}$ (cf. Sec. IV A); this can result in a smaller amplitude of the transmitted pulse if the incident pulse is short. The maximal value of the laser pulse amplitude $a_{\max}$ has to be greater than $\alpha\sqrt{2}$ for the pulse to be clearcut, say $a_{\max} \geqslant 2\alpha$. From these limitations, one can derive that for α and $a_{\max}$, the following ranges can be appropriate: $(2-3)<\alpha<(15-20)$ and $a_{\max}>2\alpha$.

For the laser pulse shaping to be effective, there is also the requirement on the growth rate of the amplitude at the front of the laser pulse. Actually, the point of the switch of transmittance just divides between the viscous and the flying regimes for the electron sheet motion. This means that when $a_0 \leqslant \alpha\sqrt{2}$, the regime is viscous, and the period of longitudinal oscillations is considerably smaller than π. To form the clearcut transmitted laser pulse, the period of the first longitudinal oscillation just after the transmittance switch should be large enough [at least greater than $(4-5)\pi$], otherwise, instead of flying, the regime for $a_0 \geqslant \alpha\sqrt{2}$ can be cutting.[22] If the cutting regime exists for some time, then the transmitted field can be close to stochastic during this time, which is inappropriate for shaping. So for effective shaping, the form of the incident laser pulse should have some point θ_s [with the amplitude $a_{0s}(\theta_s)$ of the field at this point], such that before this point, the period of the longitudinal oscillation is small and after this point it is large [for θ_s one can choose, e.g., the point with maximum derivative of $a_0(t)$]. An appropriate foil for the shaping in this case has $\alpha=a_{0s}/\sqrt{2}$. Thus, the growth rate of the amplitude for the incident laser pulse has to be large enough (at least in some interval of time) for the transmitted pulse to be clearcut.

Let us now determine the required growth rate of the incident laser pulse. We shall estimate the required value of derivative a_0' near the point θ_s, which ensures the flying regime of motion of the electron sheet after this point. For this estimation, let us suppose that the field has constant amplitude before the point θ_s, and after this point the derivative a_0' of $a_0(\theta)$ is constant,

$$a_0(\theta) = a_0; \quad \theta < \theta_s,$$
$$a_0(\theta) = a_0 + a_0'(\theta - \theta_s); \quad \theta \geqslant \theta_s. \tag{30}$$

If we use the sheet with the parameter α satisfying the equation $\alpha=a_0/\sqrt{2}$, then, before the point θ_s, the regime is viscous, so the period of longitudinal oscillations is smaller than π. In this case for the order estimate of required a_0', we can use only the second equation from the system (30), supposing that before θ_s the amplitude is equal to zero, and the jump of the amplitude in the point θ_s is equal to a_0 (this simplification allows one not to take into account the viscous regime before the flying one). Then, the integral in the expression (14) for the parameter κ can be evaluated analytically. Actually, for $a_0 \gg 1$, one has (we use the character θ instead of $\theta-\theta_s$)

$$\int_0^\theta \frac{d\theta'}{\sqrt{(a_0 + a_0'\theta')^2 + 1}} \simeq \frac{1}{a_0'} \ln\left(1 + \frac{a_0'\theta}{a_0}\right). \tag{31}$$

Let us suppose that we are interested in those θ values for which inequality $a_0'\theta<a_0$ holds. In this case, the logarithm can be approximated by the linear function, and the dependence of the parameter κ on θ is just about that for the step-like amplitude a_0 of the external pulse (also estimated for $a_0 \gg 1$). The slow (in the scale of the laser field period) part Z_s of the coordinate Z of the electron sheet can be estimated from the following equation:[22]

$$Z_s = \frac{1}{4}\int_0^\theta \frac{(a_0 + a_0'\theta)^2 d\theta}{\kappa^2 + \alpha^2} + \frac{1}{2}\int_0^\theta \frac{d\theta}{\kappa^2} - \frac{\theta}{2}. \tag{32}$$

The integral (32) can be calculated analytically. However, for the sake of simplicity, it is possible to omit the second term on the right-hand side (rhs) of this equation giving only small logarithmic correction to the result.[22] Besides, we need only order estimates, so let us suppose that a_0' is not very large (actually, smaller than 1) and $\alpha \gg \kappa_0$. In this case, one has

$$Z_s = \frac{\theta}{2}\left(\frac{a_0^2}{2\alpha^2\left(1 + \dfrac{\theta}{a_0}\right)} - 1\right) + \frac{a_0^3 a_0'}{2\alpha^2}\left[\ln\left(1 + \frac{\theta}{a_0}\right) - \frac{\theta}{a_0 + \theta}\right]. \tag{33}$$

In this expression, the terms in the first brackets on the rhs represent the result[22] for the step-like laser pulse envelope a_0, and the second-bracket terms give the correction due to the nonzero derivative a_0' of the pulse envelope. Expanding these correcting terms into the Taylor series of θ/a_0 up to the second order, one has for Z_s

This article is copyrighted as indicated in the article. Reuse of AIP content is subject to the terms at: http://scitation.aip.org/termsconditions. Downloaded to IP: 114.70.7.203 On: Wed, 12 Nov 2014 01:21:14

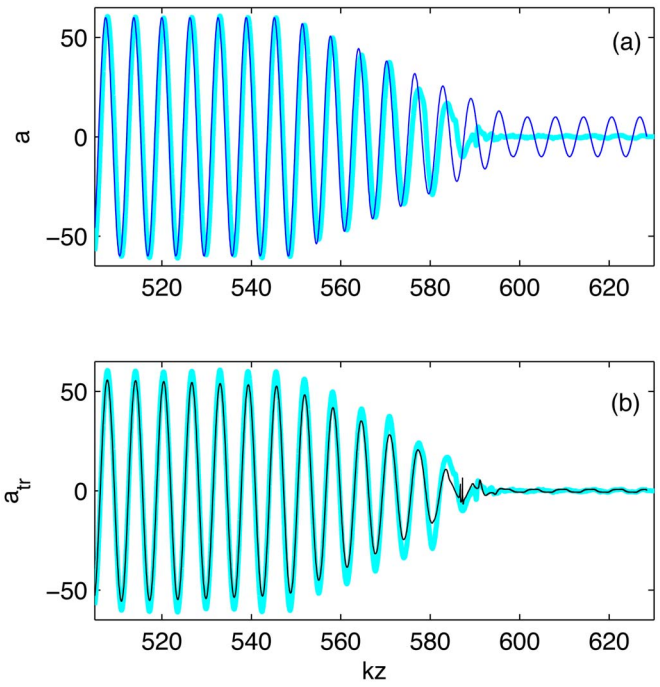

FIG. 5. (Color online) Removing the laser pulse pedestal with the electron sheet: thin blue line in (a) is the field of the incident laser pulse, thick cyan line in (a) and (b) is the transmitted field obtained in the XOOPIC simulations, thin black line in (b) is the numerical solution of Eqs. (4) and (12). The amplitude of the pedestal is $a_0=10$, the derivative $a_0'=1$, the maximal amplitude is $a_{\max}=60$, and $\alpha=15$ ($\varphi_0=0$).

$$Z_s=\frac{\theta}{2}\left(\frac{a_0^2}{2\alpha^2\left(1+\frac{\theta}{a_0}\right)}-1+\frac{a_0a_0'\theta}{2\alpha^2}\right). \tag{34}$$

The new period θ_{ld} of the longitudinal oscillations is defined by the equation $Z_s=0$. Retaining the correction terms to the linear order in θ/a_0, one has

$$\theta_{ld}\simeq\frac{a_0\left(\frac{a_0^2}{2\alpha^2}-1\right)}{1-\frac{a_0^2a_0'}{2\alpha^2}}=\frac{\theta_l}{1-\frac{a_0^2a_0'}{2\alpha^2}}. \tag{35}$$

So the nonzero derivative of the pulse envelope $a_0(\theta)$ increases the period of longitudinal oscillations of the electron sheet. However, for the increase by about two times, the required value of a_0' has to be about 0.5 for the parameters a_0 and α, satisfying the equation $\alpha=a_0/\sqrt{2}$ [this is the requirement for the transmittance switch to be in θ_s, cf. Eq. (30)]. The greater increase in the period of longitudinal oscillations requires an even larger value of a_0'. Therefore, the effective nonlinear shaping with the electron sheets is possible only for the pulses, which have at some time a sufficiently steep front ($a_0'\geqslant 0.5$).

According to these considerations, the shaping of the laser pulses with the electron sheets can be very effective, when it is necessary to remove a long pedestal of the pulse, and there is a clear transition from the pedestal to the main pulse. In Fig. 5, the shaping of such a laser pulse is presented. The form of the incident pulse is shown in Fig. 5(a) (thin blue line), the transmitted pulse simulated with the XOOPIC is presented in Fig. 5(a) and 5(b) (thick cyan line), and the field calculated with the flying mirror model is shown in Fig. 5(b) with a thin black line. The amplitude of the initial pulse pedestal is $a_0=10$, the parameter α is equal to 15, so during the pedestal the viscous regime is realized. The derivative a_0' was chosen equal to 1; the maximal laser pulse amplitude was $a_{\max}=60$.

Figure 5 shows good agreement between the PIC simulations and the numerical calculations from Eqs. (4) and (12). Again, as in the case of the step-like laser pulse envelope, the PIC simulations give a little higher transparency of the plasma layer after switching to the flying regime than the flying mirror model. On the other hand, in the viscous regime of suppression of the pedestal, the predictions of the PIC simulation coincide well with those of the flying mirror model.

So one can conclude that the suppression of the pedestal can be considerable in shaping of the laser pulses with the electron sheets, and the pedestals as high as 1/3 of the maximal laser pulse amplitude can be removed. This technique can be used also for separation of spiky features in the laser pulse from a diffuse background. The higher level of pedestal reduction can be obtained for several electron sheets (films) placed one after another at some distance. In this case, it is necessary only to choose properly the decreasing parameter α for the successive films for not to spoil the created pulse.

The shaping can be also useful for short laser pulses. In this case, the transmission through the electron sheet reduces the pulse duration. For the shaping to be effective for short pulses, the derivative of their envelope has to be greater than 0.5 (at least in some interval) similarly to the pedestal removing case. In Fig. 6, the shaping is presented for the pulse of a triangular envelope with $a_{\max}=50$ and $a_0'=2.5$ (full duration of the laser pulse is equal to 40) for $\alpha=15$, and again, the PIC simulations give reasonable agreement with the flying mirror model, especially for the shaping of the laser pulse front. At point $kz\simeq 618$ in Fig. 6, the transmission from the viscous regime to the flying regime takes place; the cutting regime is practically absent due to the fast enough growth of the laser pulse amplitude. The transmitted part of the incident pulse lies inside the first longitudinal oscillation of the electron sheet, so the transmitted pulse has a clearcut form and the shaping is effective. The front of the transmitted pulse is by more than one period shorter than that for the incident pulse. Also, due to the destruction of the plasma layer (around $kz=613$ in Fig. 6), the top and the back end of the laser pulse are transmitted through the plasma layer almost without losses. Therefore, shaping of the short laser pulses allows to generate strongly asymmetric pulses (sharp front end and considerably smoother back end), which can be effective in acceleration of the electrons in vacuum.

VI. CONCLUSIONS

The self-consistent one-dimensional flying mirror model for radiation and transmission of a thin plasma layer was

This article is copyrighted as indicated in the article. Reuse of AIP content is subject to the terms at: http://scitation.aip.org/termsconditions. Downloaded to IP: 114.70.7.203 On: Wed, 12 Nov 2014 01:21:14

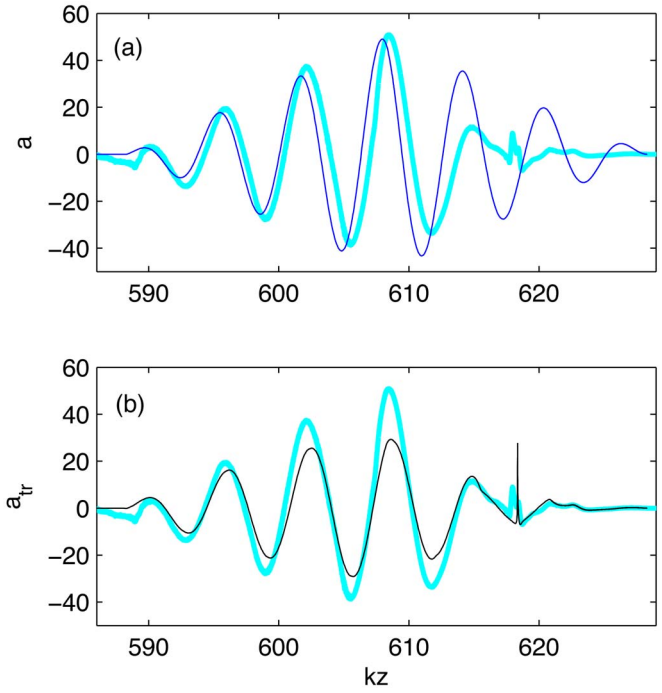

FIG. 6. (Color online) Laser pulse shortening with the electron sheet: thin blue line in (a) is the field of the incident laser pulse, thick cyan line in (a) and (b) is the transmitted field obtained in the XOOPIC simulations, thin black line in (b) is the numerical solution of Eqs. (4) and (12). The maximal amplitude of the laser pulse with triangular envelope is $a_{\max}=50$, the derivative $a_0'=2.5$ (total duration of the pulse is 40) and $\alpha=15$ ($\varphi_0=0$).

considered in this paper. This model contains one electron sheet, and it takes into account of the radiation reaction force and the Coulomb force of the ion remainder. Approximate analytical expressions for the transmitted and the reflected fields are derived for the flying mirror model. It is possible to distinguish three regimes for the transmission of the electron sheet: viscous regime, flying regime and intermediate cutting regime. For small amplitudes $a_0 \leqslant \alpha$ of the incident laser pulse, corresponding to the viscous regime of the electron sheet motion, the transmitted pulse is suppressed proportionally to the value of α, so for large α, the electron sheet is almost opaque. The reflected field in this case is sinusoidal (poor in harmonics) for $a_0 \ll \alpha$ and resembles the incident field, while for $a_0 \approx \alpha$ the transmitted and the reflected fields are enriched with harmonics.

The transmission of the electron sheet in the flying regime, when $a_0 \gg \alpha\sqrt{2}$, is not only amplitude-dependent, but also time-dependent (the electron sheet protracts the sharp laser front), and for long enough incident laser pulses, the transmission can be close to unity. Besides, the amplitude transmission coefficient depends essentially on the form of the laser pulse envelope. The transmitted pulse is poor in harmonics in the flying regime, while the reflected field for the electron sheet has a wide spectral band. Between the viscous and the flying regimes, the intermediate cutting regime is situated. In this regime, the transmitted and the reflected fields look like a stochastic sample.

To check the validity of results, the predictions of the flying mirror model were compared with the predictions of the sliding mirror model[1–3] and the pure Coulomb model,[22] and also, with the 1D PIC simulations. This comparison shows that the flying mirror model is more adequate than other models for the description of the transmittance of real thin plasma layers in a high laser pulse amplitude regime.

Dependence of the electron sheet transmission on the incident pulse amplitude can be used for the shaping of the laser pulses. The two most appropriate applications here include the removal of the laser pulse pedestal and the reduction of the length for the short laser pulses. The suppression of the pedestal is about $1/\alpha$, and pedestals up to $1/3$ of the maximal field amplitude can be suppressed. This effect allows to separate spiky features in the laser pulse from a diffuse background. For the reduction of the pulse length to be effective, laser pulse should have steep enough front [large value of $a_0'(t)$]; after shaping, the asymmetric pulses with sharp front end and smooth back end are generated. These results were compared with the 1D PIC simulations and the good agreement was established. The transmission of the plasma layer in the PIC simulations shows even higher values for the peak amplitudes than in the flying mirror model due to the destruction of the layer.

ACKNOWLEDGMENTS

We thank S. V. Bulanov for stimulating discussions and valuable comments. This work was supported by the Creative Research Initiative Program of the Korean Ministry of Science and Technology.

[1] S. V. Bulanov, T. J. Esirkepov, N. M. Naumova, F. Pegoraro, I. V. Pogorelsky, and A. M. Pukhov, IEEE Trans. Plasma Sci. **24**, 393 (1996).
[2] S. V. Bulanov, A. Macchi, and F. Pegoraro, Phys. Lett. A **245**, 439 (1998).
[3] V. A. Vshivkov, N. M. Naumova, F. Pegoraro, and S. V. Bulanov, Phys. Plasmas **5**, 2727 (1998).
[4] K. Nagashima, Y. Kishimoto, and H. Takuma, Phys. Rev. E **58**, 4937 (1998).
[5] V. V. Goloviznin and T. J. Schep, Phys. Plasmas **7**, 1564 (2000).
[6] R. A. Cairns, B. Rau, and M. Airila, Phys. Plasmas **7**, 3736 (2000).
[7] B. Shen and Z. Xu, Phys. Rev. E **64**, 056406 (2001).
[8] B. Shen and J. Meyer-ter-Vehn, Phys. Plasmas **8**, 1003 (2001).
[9] A. Zhidkov, J. Koga, A. Sasaki, and M. Uesaka, Phys. Rev. Lett. **88**, 185002 (2002).
[10] Y. Sentoku, T. E. Cowan, A. Kemp, and H. Ruhl, Phys. Plasmas **10**, 2009 (2003).
[11] Sh. Amiranashvili, M. Y. Yu, and L. Stenflo, Phys. Plasmas **10**, 1239 (2003).
[12] G. A. Mourou, C. P. J. Barty, and M. D. Perry, Phys. Today **51**(1), 22 (1998).
[13] D. Giulietti, L. A. Gizzi, A. Giulietti, A. Macchi, D. Teychenne, P. Chessa, A. Rousse, G. Cheriaux, J. P. Chambaret, and G. Darpentigny, Phys. Rev. Lett. **79**, 3194 (1997).
[14] J. Fuchs, J. C. Adam, F. Amiranoff *et al.*, Phys. Plasmas **6**, 2569 (1999).
[15] Y. T. Li, J. Zhang, L. M. Chen *et al.*, Phys. Rev. E **64**, 046407 (2001).
[16] P. Audebert, R. Shepherd, K. B. Fournier, O. Peyrusse, D. Price, R. W. Lee, P. Springer, J.-C. Gauthier, and L. Klein, Phys. Rev. E **66**, 066412 (2002).
[17] U. Teubner, K. Eidmann, U. Wagner, U. Andiel, F. Pisani, G. D. Tsakiris, K. Witte, J. Meyer-ter-Vehn, T. Schlegel, and E. Forster, Phys. Rev. Lett. **92**, 185001 (2004).
[18] R. Lichters, J. Meyer-ter-Vehn, and A. Pukhov, Phys. Plasmas **3**, 3425 (1996).
[19] D. Von der Linde and K. Rzazewski, Appl. Phys. B: Lasers Opt. **63**, 499 (1996).
[20] A. S. Pirozhkov, S. V. Bulanov, T. Zh. Esirkepov *et al.*, Phys. Lett. A **349**, 256 (2006).
[21] A. S. Pirozhkov, S. V. Bulanov, T. Zh. Esirkepov, M. Mori, A. Sagisaka, and H. Daido, Phys. Plasmas **13**, 013107 (2006).

This article is copyrighted as indicated in the article. Reuse of AIP content is subject to the terms at: http://scitation.aip.org/termsconditions. Downloaded to IP: 114.70.7.203 On: Wed, 12 Nov 2014 01:21:14

[22]V. V. Kulagin, V. A. Cherepenin, M. S. Hur, and H. Suk, Phys. Plasmas **14**, 113101 (2007).
[23]S. V. Bulanov, T. Esirkepov, and T. Tajima, Phys. Rev. Lett. **91**, 085001 (2003).
[24]C. K. Birdsall and A. B. Langdon, *Plasma Physics Via Computer Simulation* (MacGraw-Hill Book Company, New York, 1985), p. 8.
[25]V. A. Cherepenin, A. S. Il'in, and V. V. Kulagin, Fiz. Plazmy **27**, 1111 (2001) [Plasma Phys. Rep. **27**, 1048 (2001)].
[26]A. S. Il'in, V. V. Kulagin, and V. A. Cherepenin, Radiotekh. Elektron. (Moscow) **44**, 389 (1999) [J. Commun. Technol. Electron. **44**, 385 (1999)].
[27]S. V. Bulanov, V. A. Vshivkov, G. I. Dudnikova *et al.*, in *Problems of Plasma Theory*, edited by V. D. Shafranov (Kluwer, Dordrecht, 2001).
[28]H. Usui, J. P. Verboncoeur, and C. K. Birdsall, IEICE Trans. Electron. **E83C**, 989 (2000).
[29]V. V. Kulagin, V. A. Cherepenin, and H. Suk, Phys. Plasmas **11**, 5239 (2004).
[30]V. V. Kulagin and H. Suk, J. Korean Phys. Soc. **44**, 1282 (2004).

This article is copyrighted as indicated in the article. Reuse of AIP content is subject to the terms at: http://scitation.aip.org/termsconditions. Downloaded to IP: 114.70.7.203 On: Wed, 12 Nov 2014 01:21:14